engineering proceedings

MDPI

Proceeding Paper

The Fabrication of Porous ZnO Nanorods through Two-Step Aqueous Synthesis, and Their Properties †

Chih-Feng Yen *, Hung-Chang Hsu, Chung-Hung Lin, Yu-De Lin and Shih-Fong Chao *

Department of Microelectronics Engineering, National Kaohsiung University of Science and Technology, No. 142, Haizhuan Rd., Nanzi Dist., Kaohsiung City 811213, Taiwan; f110187113@nkust.edu.tw (H.-C.H.); f110187118@nkust.edu.tw (C.-H.L.); f110187105@nkust.edu.tw (Y.-D.L.)

* Correspondence: cfyen@nkust.edu.tw (C.-F.Y.); sfchao@nkust.edu.tw (S.-F.C.); Tel.: +886-7-3617141 (ext. 23374) (C.-F.Y.); +886-7-3617141 (ext. 23365) (S.-F.C.)

† Presented at the 3rd IEEE International Conference on Electronic Communications, Internet of Things and Big Data Conference 2023, Taichung, Taiwan, 14–16 April 2023.

Abstract: In this study, ZnO nanorods with a porous structure were successfully prepared using the chemical bath deposition (CBD) method. According to the surface and cross-sectional images photographed by scanning electron microscopy, we found that the diameters of samples with concentrations of 10, 30, 50, and 70 mM were 90, 141, 214, and 259 nm, respectively, with 6 h of deposition. The height of the nanorods was maintained at approximately 1.3 μm. The EDS material analysis showed that the ratio of zinc atoms and oxygen atoms in samples with different concentrations changed with the concentration of the growth solution. The column diameter of the zinc oxide nanorods prepared by the chemical bath deposition method was closely related to the concentration of the growth solution. The higher the concentration, the larger the column diameter. The height of the nanorods was directly proportional to the deposition time and was not influenced by solution concentration.

Keywords: CBD; ZnO nanorods; porous; zinc oxide

Citation: Yen, C.-F.; Hsu, H.-C.; Lin, C.-H.; Lin, Y.-D.; Chao, S.-F. The Fabrication of Porous ZnO Nanorods through Two-Step Aqueous Synthesis, and Their Properties. *Eng. Proc.* **2023**, *38*, 79. https://doi.org/10.3390/engproc2023038079

Academic Editors: Teen-Hang Meen, Hsin-Hung Lin and Cheng-Fu Yang

Published: 10 July 2023

1. Introduction

With the development of technology and the evolution of the semiconductor industry, the requirements for the integration of integrated circuits are higher, and the evolution of materials has moved from the micron level to the nanometer level. However, zinc oxide (ZnO) has attracted much attention and is one of the most widely used metal materials. Zinc oxide has three types of crystallite structures, rock salt structure, sphalerite, and hexagonal wurtzite [1]. The most stable structure of zinc oxide is the hexagonal wurtzite structure; this has a forbidden band width of 3.37 eV, and a large exciton binding energy of 60 MeV [2,3]. In the semiconductor industry, due to its high oxidizing power, stability, and low toxicity, zinc oxide is widely used. At present, the common preparation methods of zinc oxide include metal–organic chemical vapor deposition (MOCVD) [4], molecular beam epitaxy (MBE) [5], pulsed excimer vapor deposition (PVD) [6], vapor-phase epitaxy (VPE) [7], the physical vapor transport method (VPT) [8], and the gas–liquid–solid-phase method (VLS) [9].

Zinc oxide is a material that has been widely used to make inexpensive, non-toxic, and high-performance photocatalysts, to degrade a wide variety of organic chemicals and organic dyes [10]. It can be used in ceramics, gas sensing, light sensing, photocatalyst, and other applications. Nanorods (NRs) are one-dimensional structures of nanomaterials, and zinc oxide nanorods are more outstanding in the above-mentioned aspects.

The seed layers of zinc oxide were successfully prepared using the sol–gel method, and the ZnO nanorods were built by the non-vacuum chemical bath deposition method to prepare uniformly distributed and porous ZnO nanorods. These pores can expand

the specific surface area, being very useful for photocatalytic reactions and gas-sensing detection [11].

2. Experimental Section

P-Si(100) was chosen as the substrate in this study. First, the silicon substrate was cleaned with DI water, acetone, and ethanol by ultrasonic shock for 10 min in sequence, and then shock-washed with DI water again to remove the surface of the substrate residual ethanol. Finally, blow drying with nitrogen was performed to remove moisture. The experiment consisted of two parts: (a) the seed layer of zinc oxide was prepared on a silicon substrate by the sol–gel method and spin coater to form a seed layer; (b) ZnO NRs were deposited on the seed layer by non-vacuum chemical bath deposition.

Subsequently, 0.01 mol of $Zn(CH_3COO)_2{\cdot}2H_2O$ and appropriate amounts of $CH_3OCH_2CH_2OH$ were fully stirred at 60 °C for 20 min; then, $NH_2CH_2CH_2OH$ was slowly added as a stabilizer for the reaction, and after stirring at the same temperature for 2 h, the solution was aged at 25 °C for 24 h. The preparation steps of the seed layer growth solution are shown in Figure 1. A seed layer was prepared using a spin coater; spin-coating was performed at 3000 rpm for 30 s; and then soft-baking was performed. The process was repeated 3 times to ensure that the seed layer was successfully attached to the silicon substrate, and finally placed in a high-temperature quartz furnace tube for annealing at 500 °C for 2 h.

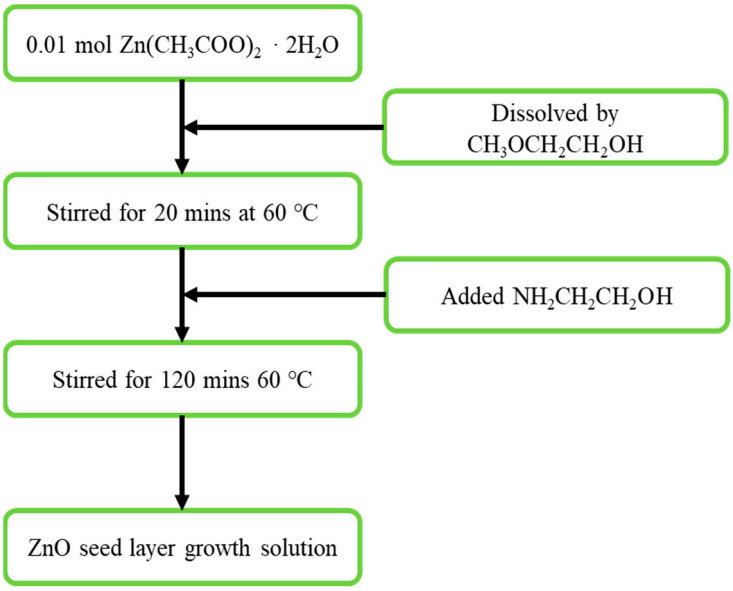

Figure 1. Seed layer growth solution preparation.

The zinc oxide nanorod growth solution used in the liquid deposition method was prepared by mixing $Zn(NO_3)_2 \cdot 6H_2O$ and $C_6H_{12}N_4$ (HMT). First, an appropriate amount of $Zn(NO_3)_2 \cdot 6H_2O$ was stirred with deionized water for 20 min. HMT was stirred with deionized water at the same time. Then, the mixed growth solution was placed in a constant-temperature water bath for 20 min at 90 °C to preheat; then, the silicon substrate with the seed layer was completely deposited in the growth solution for 6 h. After deposition, the samples were taken out and cleaned with deionized water, and the chemical reaction was terminated. After drying with N_2, the deposited zinc oxide nanorods were annealed at 500 °C for 2 h in a high-temperature quartz furnace tube with air. Finally, the annealed samples were subjected to surface analysis and material composition detection. The preparation steps of the NR layer growth solution are shown in Figure 2.

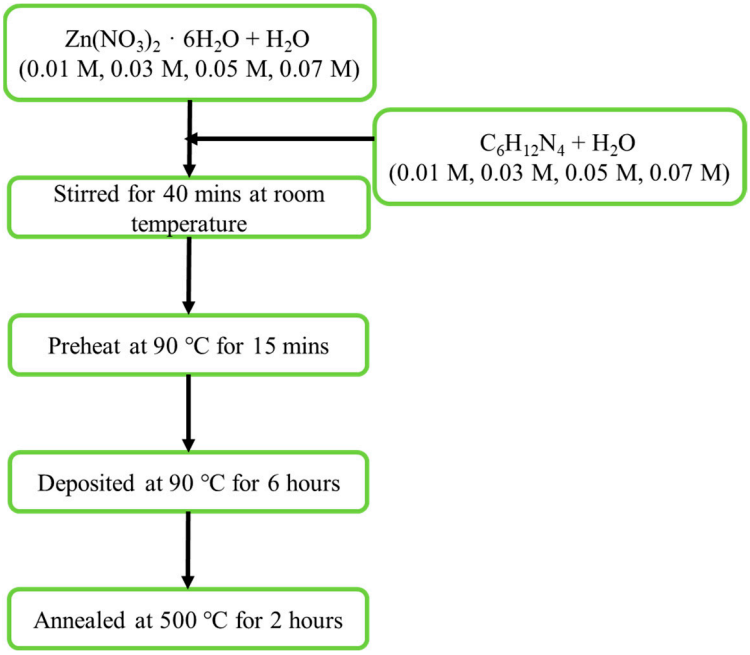

Figure 2. Nanorod growth solution preparation.

When the nanorods were initially deposited, HMT began to decompose into ammonia and produced hydroxide ions or OH^-; the detailed reaction is shown in Formula (1) and (2) [12]:

$$(CH)_6N_4 + 6H_2O \rightarrow 6HCHO + NH_3 \quad (1)$$

$$H_2O + NH_3 \boxplus OH^- + NH^{4+} \quad (2)$$

The reactive formation of the ZnO core is due to the reaction of Zn^{2+} cations with NH_3 and OH^- anions; the detailed reaction is depicted in Formula (3) [13]:

$$Zn^{2+} + 2OH^- \rightarrow Zn(OH)_2 \text{ or } Zn(NH_3)_4{}^{2+} + 2OH^- \rightarrow Zn(OH)_2(NH_3)_4 \quad (3)$$

Under the influence of specific temperatures and OH ions, the crystal core degrades into ZnO core nanorods. Over time, the ZnO core grows and finally forms nanorods, as detailed by the reaction in Formula (4) [13]:

$$Zn(OH)_2 \rightarrow ZnO + H_2O \text{ or } Zn(OH)_2(NH_3)_4 \rightarrow ZnO + H_2O + 4NH_3 \quad (4)$$

3. Results and Discussion

In this study, the porous nanorods of zinc oxide were successfully deposited on the silicon substrate using the chemical bath deposition method. The material composition was confirmed by EDS. Whether the concentration of the growth solution was related to the change in the surface appearance of the NRs was confirmed by cross-sectional SEM images.

According to the EDS composition analysis results, it can be determined that the nanorods in those samples were composed of Zn atoms and O atoms. The proportion of O atoms in the ZnO nanorod sample accounted for 44.77%, and the proportion of Zn atoms accounted for 55.23%, as shown in Figure 3a. The proportion of O atoms in the ZnO nanorod sample accounted for 47.15%, and the proportion of Zn atoms accounted for 52.85%, as shown in Figure 3b. According to the above results, the ratio of oxygen atoms to zinc atoms changed with the concentration of the growth solution.

Figure 4a–h show the SEM images of ZnO NRs under different concentrations of growth solution. The reason why the liquid-phase deposition method can grow ZnO nanorods is due to the higher surface energy of zinc oxide along the [0001] direction, which will have a higher growth rate. Figure 4a–d show high-magnification images (magnification

20 K) of samples with concentrations of 10, 30, 50, and 70 mM, respectively; Figure 4e–h are the top views of samples with corresponding concentrations. The image in Figure 4 shows that all grown ZnO nanorods were also in the shape of hexagonal columns, and most of the ZnO nanorods grew vertically upward. The column diameters of the nanorods of zinc oxide were 90, 141, 214, and 259 nm, respectively. This shows that the column diameter of the grown nanorods of zinc oxide increased when the concentration of the growth solution increased. The higher the concentration of the growth solution, the faster the growth rate in the [0001] direction. Many small pores can be observed from the surface of the sample, which is likely to be caused by the high-temperature gasification of acetate ions and intermediate reactants in the sample during the annealing process. The specific surface area of the meter column is beneficial for photocatalysis.

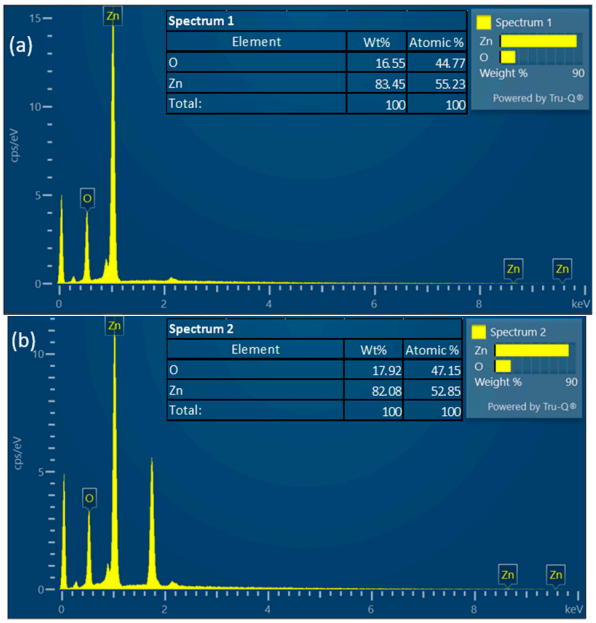

Figure 3. EDAX spectrum of ZnO NRs: (**a**) 10 mM and (**b**) 50 mM.

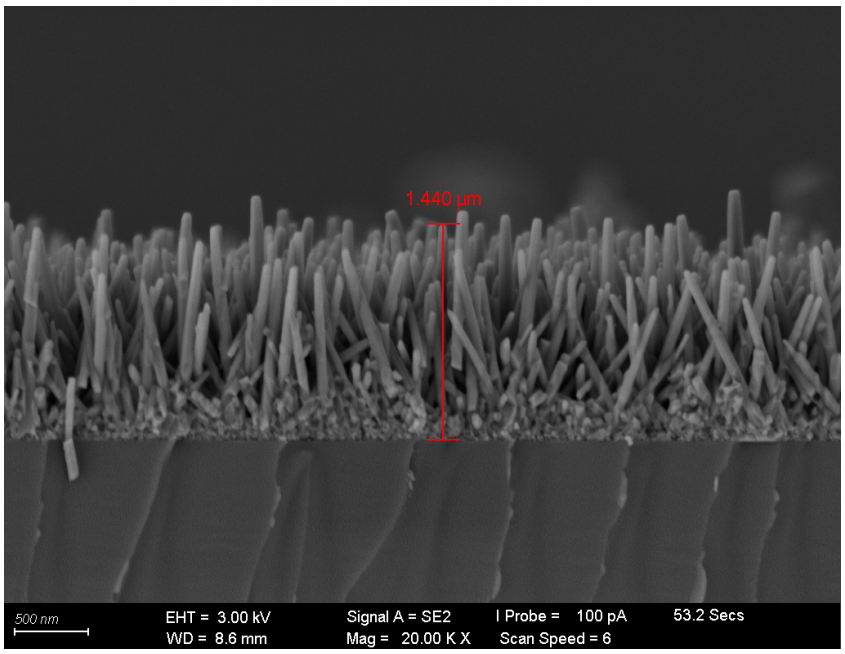

(**a**) 10mM sample ZnO NRs SEM Cross-section

Figure 4. *Cont.*

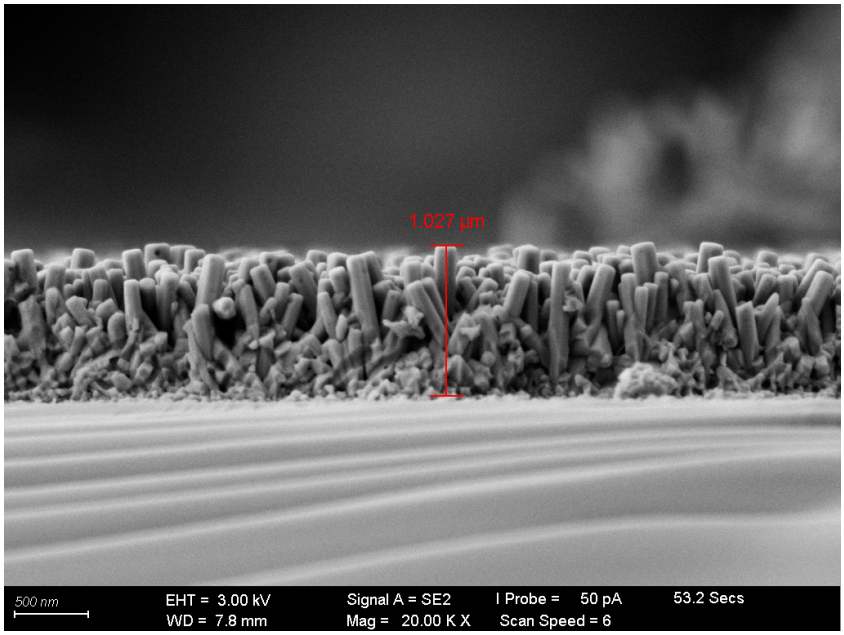

(**b**) 30mM sample ZnO NRs SEM Cross-section

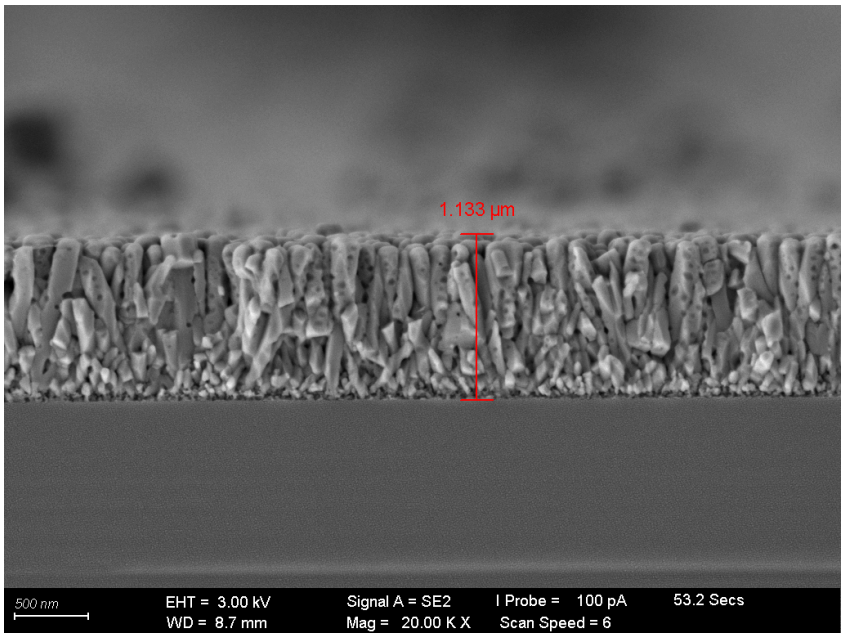

(**c**) 50mM sample ZnO NRs SEM Cross-section

Figure 4. *Cont.*

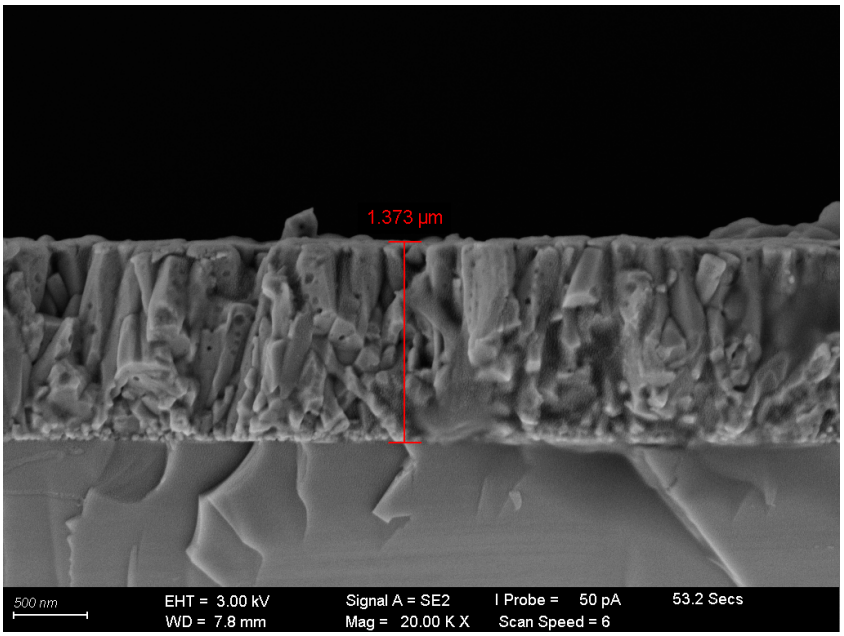

(**d**) 70mM sample ZnO NRs SEM Cross-section

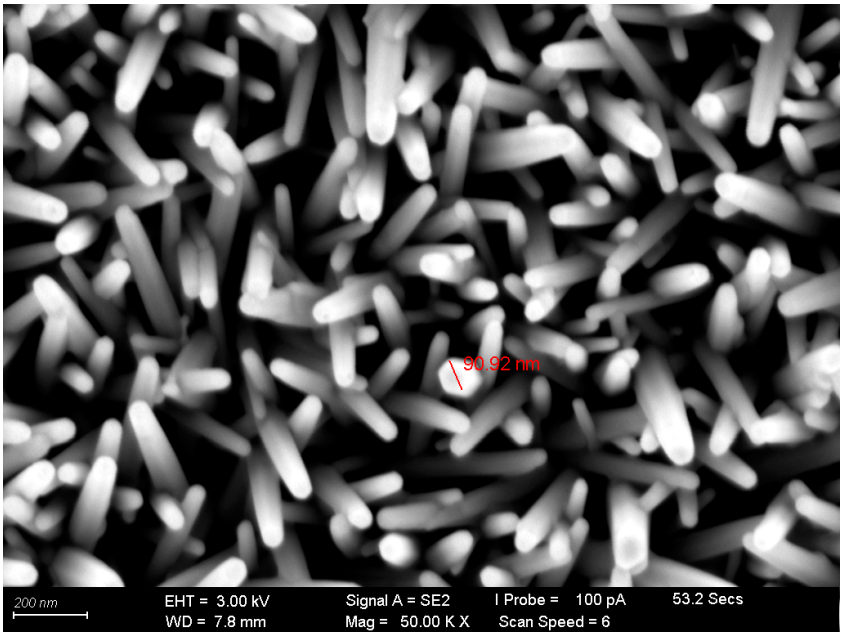

(**e**) 10mM sample ZnO NRs SEM Top View

Figure 4. *Cont*.

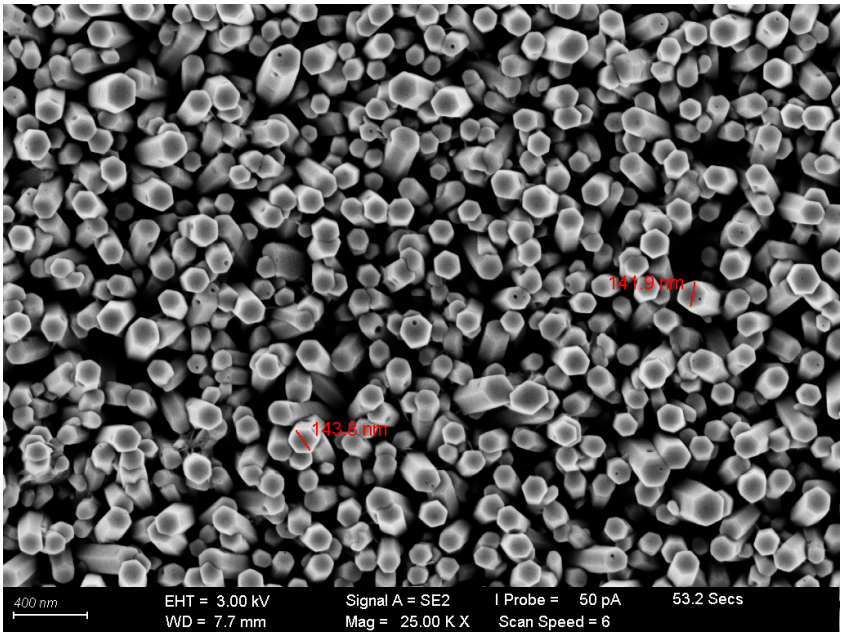

(**f**) 30mM sample ZnO NRs SEM Top View

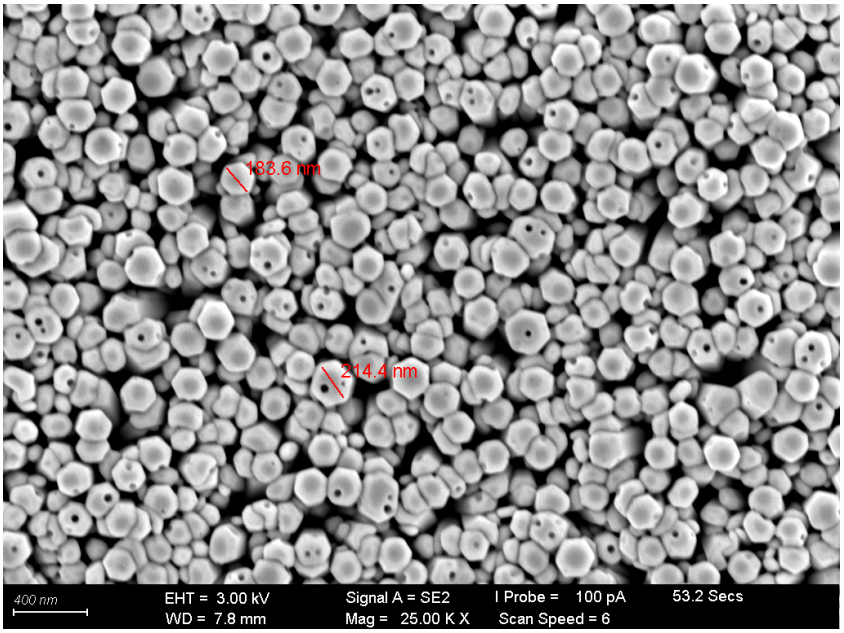

(**g**) 50mM sample ZnO NRs SEM Top View

Figure 4. *Cont.*

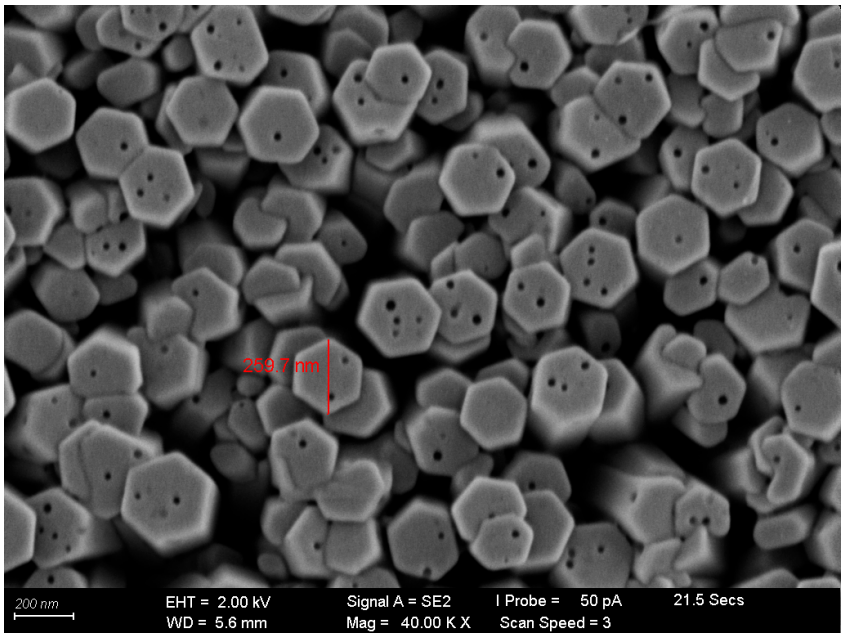

(**h**) 70mM sample ZnO NRs SEM Top View

Figure 4. FE-SEM images of ZnO NRs with different concentrations of growth solution: (**a**,**e**) 10 mM; (**b**) and (**f**) 30 mM; (**c**) and (**g**) 50 mM; (**d**) and (**h**) 70 mM.

4. Conclusions

In this study, the chemical bath method and subsequent annealing process were used to successfully prepare porous zinc oxide nanorod arrays on the P-Si(100) substrate. According to the SEM images, it was found that the samples of 10 mM, 30 mM, 50 mM, and 70 mM were deposited over 6 hours; the column diameters were 90 nm, 141 nm, 214 nm, and 259 nm, respectively. The height of the nanorods was maintained at about 1.3 μm. This indicates that the growth solution of zinc oxide nanorods prepared by the chemical bath deposition method will affect the diameter of ZnO NRs, and the height of ZnO NRs is related to the deposition time rather than the concentration of the growth solution. Additionally, according to the EDS material analysis, it was found that nanorods grown from growth solutions with different concentrations were composed of different ratios of zinc atoms and oxygen atoms. The pores created by annealing greatly increased the specific surface area of the nanorods, making them advantageous for future applications in photocatalysis.

Author Contributions: Conceptualization, C.-F.Y. and H.-C.H.; methodology, C.-F.Y.; software, H.-C.H.; validation, C.-F.Y., S.-F.C. and H.-C.H.; formal analysis, H.-C.H.; investigation, H.-C.H.; resources, H.-C.H., C.-H.L. and Y.-D.L.; data curation, H.-C.H.; writing—original draft preparation, H.-C.H.; writing—review and editing, C.-F.Y.; visualization, C.-F.Y.; supervision, C.-F.Y. and S.-F.C.; project administration, C.-F.Y. and S.-F.C.; funding acquisition, C.-F.Y. and S.-F.C. All authors have read and agreed to the published version of the manuscript.

Funding: This research received no external funding.

Institutional Review Board Statement: Not applicable.

Informed Consent Statement: Not applicable.

Data Availability Statement: Not applicable.

Conflicts of Interest: The authors declare no conflict of interest.

References

1. Chinnasamy, M.; Balasubramanian, K. Enhanced UV photodetection behavior of Cr doped wurtzite ZnO crystalline nanorods. *Opt. Mater.* **2020**, *110*, 110492. [CrossRef]
2. Liu, B.; Zeng, H.C. Hydrothermal Synthesis of ZnO Nanorods in the Diameter Regime of 50 nm. *J. Am. Chem. Soc.* **2003**, *125*, 4430–4431. [CrossRef] [PubMed]
3. Jiang, Z.-Y.; Xu, T.; Xie, Z.-X.; Lin, Z.-W.; Zhou, X.; Xu, X.; Huang, R.-B.; Zheng, L.-S. Molten Salt Route toward the Growth of ZnO Nanowires in Unusual Growth Directions. *J. Phys. Chem. B* **2005**, *109*, 23269–23273. [CrossRef] [PubMed]
4. Wu, B.; Zhang, Y.; Shi, Z.; Li, X.; Cui, X.; Zhuang, S.; Zhang, B.; Du, G. Different defect levels configurations between double layers of nanorods and film in ZnO grown on c-Al2O3 by MOCVD. *J. Lumin.* **2014**, *154*, 587–592. [CrossRef]
5. Tien, L.; Norton, D.; Pearton, S.; Wang, H.; Ren, F. Nucleation control for ZnO nanorods grown by catalyst-driven mo-lecular beam epitaxy. *Appl. Surf. Sci.* **2007**, *253*, 4620–4625. [CrossRef]
6. Kek, R.; Ong, G.; Yap, S.; Lim, L.; Koh, S.; Nee, C.; Tou, T.; Yap, S. Growth of Al-doped ZnO nanostructures in low pres-sure background gas by pulsed laser deposition. *Mater. Sci. Semicond. Process.* **2022**, *145*, 106636. [CrossRef]
7. Maejima, K.; Ueda, M.; Fujita, S.; Fujita, S. Growth of ZnO Nanorods on A-Plane (1120) Sapphire by Metal-Organic Vapor Phase Epitaxy. *Jpn. J. Appl. Phys.* **2003**, *42*, 2600–2604. [CrossRef]
8. Gray, C.; Trefflich, L.; Röder, R.; Ronning, C.; Henry, M.O.; McGlynn, E. Growth of 18 O isotopically enriched ZnO nanorods by two novel VPT methods. *J. Cryst. Growth* **2017**, *460*, 85–93. [CrossRef]
9. Suh, D.-I.; Byeon, C.C.; Lee, C.-L. Synthesis and optical characterization of vertically grown ZnO nanowires in high crystallinity through vapor–liquid–solid growth mechanism. *Appl. Surf. Sci.* **2010**, *257*, 1454–1456. [CrossRef]
10. Irani, M.; Mohammadi, T.; Mohebbi, S. Photocatalytic Degradation of Methylene Blue with ZnO Nanoparticles; a Joint Experimental and Theoretical Study. *J. Mex. Chem. Soc.* **2016**, *60*, 218–225.
11. Duan, X.; Li, C.; Fu, L.; Wu, Y.; Chen, G.; Xu, K.; Shao, L.; Yang, P.; Yu, Z.; Ding, P.; et al. Structural and optical properties of porous ZnO nanorods synthesized by a simple two-step method. *Superlattices Microstruct.* **2019**, *128*, 30–36. [CrossRef]
12. Kumar, V.; Gupta, R.; Bansal, A. Hydrothermal Growth of ZnO Nanorods for Use in Dye-Sensitized Solar Cells. *ACS Appl. Nano Mater.* **2021**, *4*, 6212–6222. [CrossRef]
13. Ichikawa, T.; Shiratori, S. Fabrication and Evaluation of ZnO Nanorods by Liquid-Phase Deposition. *Inorg. Chem.* **2010**, *50*, 999–1004. [CrossRef] [PubMed]